JOC The Journal of Organic Chemistry

Article

pubs.acs.org/joc

Evidence of Nanotubular Self-Organization in Solution and Solid States of Heterochiral Cyclo 1:1 [α/α-N^{α}-Bn-hydrazino]mers Series

Ralph-Olivier Moussodia,[†] Samir Acherar,*[,†] Eugénie Romero,[†] Claude Didierjean,[‡] and Brigitte Jamart-Grégoire*[,†]

[†]Laboratoire de Chimie Physique Macromoléculaire (LCPM), Université de Lorraine-CNRS, UMR 7375, 1 rue Grandville, BP 20451, 54001 Nancy cedex, France

[‡]Laboratoire de Crystallographie, Résonance Magnétique et Modélisations (CRM2), Université de Lorraine-CNRS, UMR 7036, Faculté des Sciences et Technologies, BP 20239, 54506 Vandœuvre-lès-Nancy cedex, France

Supporting Information

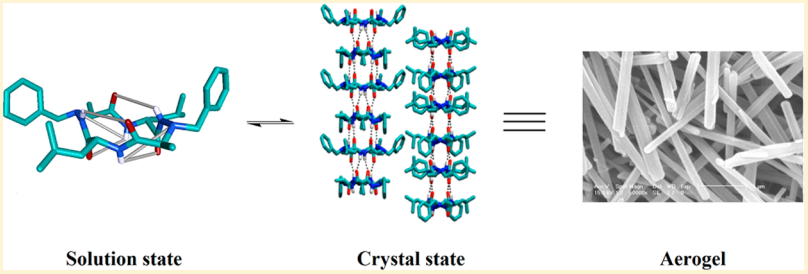

ABSTRACT: The cyclization of heterochiral 1:1 [α/α-N^{α}-Bn-hydrazino]mers leads to the corresponding cyclotetramer and cyclohexamer **3** and **4**. X-ray crystallographic analysis of **3** unveils its ability to self-assemble into nanotubular structures. Further experiments conducted in the solid state through SEM analyses demonstrate the capability of **3** and **4** to form aerogels consisting of a network of nontwisted fibers, thus confirming the presence of self-organization within this series of mixed-hydrazinopeptides. Subsequent FTIR and NMR studies demonstrate the presence of an equilibrium between monomeric (intramolecular H-bonds) and nanotubular (intermolecular H-bonds) forms in solution. This equilibrium can be modified by varying the solvent.

INTRODUCTION

The organization of shape-persistent peptidic macrocycles into supramolecular structures has gained considerable interest because of the modularity of their surface and internal diameter, which can be tuned by the choice of the individual subunits and the length of the amino acid chain. These noteworthy features make them good candidates for potential applications in nanomedicine, biotechnologies, and material science.[1−3]

Hassall was the first to envision the formation of theses tubular assemblies, called nanotubes, through the self-assembly of cyclic subunits by noncovalent processes (e.g., H-bonding, aromatic stacking) in 1972.[4] He suggested that cyclic tetramers of alternating α- and β-amino acids would assemble through backbone−backbone H-bonding to form hollow cylindrical structures. This prediction was only partially validated in 1974 by a crystallographic analysis of the tetrapeptide cyclo[−(L-Ser(OtBu)-β-Ala-Gly-β-Asp(OMe))−].[5] Indeed, the peptides were shown to organize as rings that stacked above one another in the crystal cell. However, only two of the four amide groups engaged in the expected inter-subunit H-bonds. During the same year, within the context of a theoretical analysis of peptide sequences, De Santis et al.[6] concluded that peptides comprising an even number of alternating D- and L-amino acid residues, which display conformationally equivalent β-type dihedral angles, would form closed rings capable of stacking through backbone−backbone H-bonding, leading to a contiguous sheet structure. However, Ghadiri and co-workers were the first to assemble cyclic peptide into a nanotube in 1993, which they achieved by controlled acidification of a pH-responsive octapeptide.[7]

More recently, the concept of peptidic nanotubes has been extended to cyclic pseudopeptides containing β-amino acids,[8−11] alternating α- and β-amino acids (14-membered ring),[5] vinylogous δ-amino acids (18-membered ring),[12] and oligoureas.[13,14] Among these pseudopeptidic macrocycles, a new class has been highlighted: the hydrazinopeptides. These pseudopeptides differ from regular peptides through the replacement of the amide bond by a hydrazide bond, extending the concept of β-peptides (Figure 1a).[15,16] Thanks to the presence of a supplementary nitrogen, these α-hydrazinopeptides offer a wide variety of possible structure modifications and novel types of secondary structure.

Le Grel and co-workers recently demonstrated that aza-β^3-cyclopeptides (i.e. hydrazinoglycine oligomers) could be obtained from the corresponding linear oligomers.[17,18] X-ray crystallographic and NMR analyses showed that the cyclic aza-

Received: November 27, 2014
Published: March 3, 2015

DOI: 10.1021/jo502684g
J. Org. Chem. 2015, 80, 3022−3029

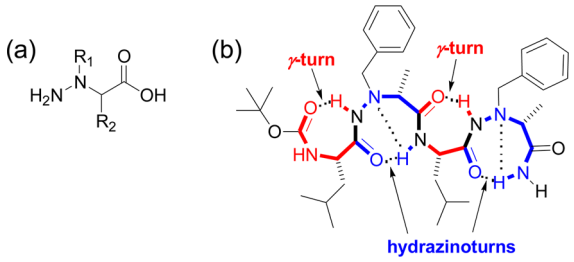

Figure 1. Bis-nitrogenated compounds: (a) hydrazino acid and (b) autostructuration of a heterochiral 1:1 [α/α-N^{α}-Bn-hydrazino] tetramer into γ-turns and hydrazinoturns.

β^3 scaffold, as its linear precursors, is structured by a fully cooperative intramolecular H-bonding network. This is in sharp contrast to the nanotubular assemblies observed for β-cyclotetrapeptides, which rely on intermolecular H-bonding.[10,19]

Moreover, we have shown previously that heterochiral linear pseudopeptides composed by the alternation of α-amino acids and α-hydrazino acids can fold in solution via a succession of γ-turns and hydrazinoturns (Figure 1b).[20] This structuration is similar to the one observed by Yang and co-workers for mixed 1:1 [α/α-aminoxy]mers, which indeed alternate γ-turns and N−O turns.[21,22]

We expect these specific conformational features to enhance macrocyclization greatly. Therefore, we propose to synthesize the corresponding macrocyclic derivatives and to evaluate their propensities to form tubular assemblies.

In comparison with the rich knowledge that has been gathered on the propensity of nanotubes to self-assemble in the solid state, less is known concerning their behavior in solution. Herein we report and compare the conformational behavior of heterochiral cyclo 1:1 [α/α-N^{α}-Bn-hydrazino]mers in the solid state, in solution, and in the gel.

RESULTS AND DISCUSSION

The general stepwise strategy used to synthesize the heterochiral cyclo 1:1 [α/α-N^{α}-Bn-hydrazino]mers **3** and **4** is described in Scheme 1. Linear heterochiral tetramer **1** and hexamer **2**, respectively, were obtained by a coupling reaction using conditions described previously.[20,23] The corresponding macrocycles **3** and **4** were obtained from the deprotected precursors by reaction with an excess of HBTU in DCM/DMF at 1 mM. They were isolated with very high purity in yields of over 35%. These yields are lower than those obtained for the cyclization of aza-β^3-peptides (over 70%) performed by Le Grel's group.[17,18] Such a discrepancy may at first be considered rather surprising because the conformations of the aza-β^3-peptides and the α/α-hydrazinopeptides likely rely on similar hydrazinoturn conformations.[20,24,25] It should be noted, however, that the lack of a chiral asymmetric carbon C^{α} confers a specific conformational flexibility to aza-β^3-peptides, a specific feature that likely plays a role in the greater efficiency of the macrocyclization.

Single crystals of **3** suitable for X-ray crystallographic analysis were grown by slow evaporation from a CH_3CN/EtOH solution (see pp S9 and S10 in the Supporting Information). Tetracycle **3** crystallized in the space group *C*2 with four half-molecules in the asymmetric unit (i.e. eight molecules in the unit cell). All of independent molecules exhibited the same C_2-symmetric conformation in which the central hole of the ring is

Scheme 1. General Stepwise Strategy for Macrocyclization of 3 and 4

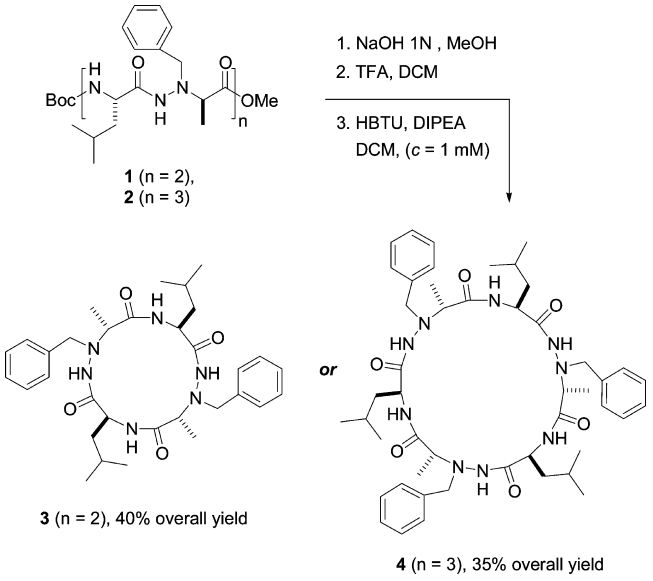

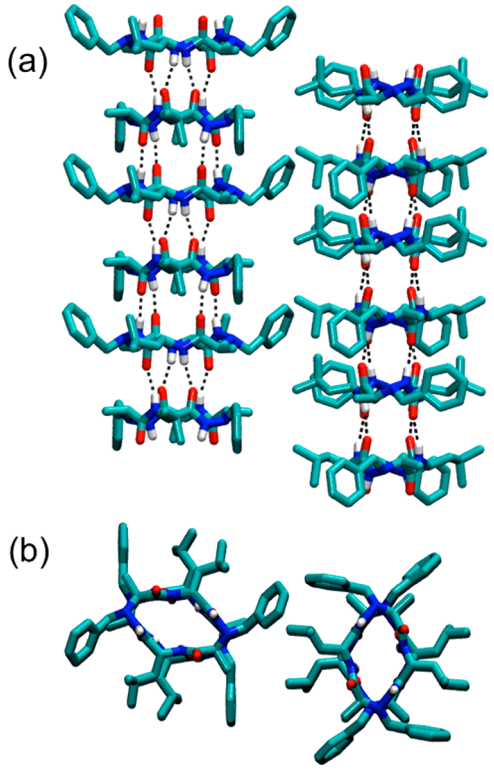

Figure 2. View of the nanotubular organization of **3** in the crystal state (X-ray): (a) side view; (b) view from the top. The intermolecular H-bonds are marked as dashed lines. The H atoms, except those of the NH groups, have been omitted for clarity.

collapsed and the substituents adopt pseudoequatorial positions. Moreover, all of the N^{α} atoms have a pyramidal conformation with the *R* configuration as C^{α} atoms of D-leucine residues. Thus, their side chains and the mean plane of the ring are practically coplanar and allow tight packing of the molecules into nanotubes. The 14-membered macrocycle shows an all-*trans* conformation, as observed in most crystal structures of α,β-cyclotetrapeptides (α,β-CTPs) described in

DOI: 10.1021/jo502684g
J. Org. Chem. 2015, 80, 3022−3029

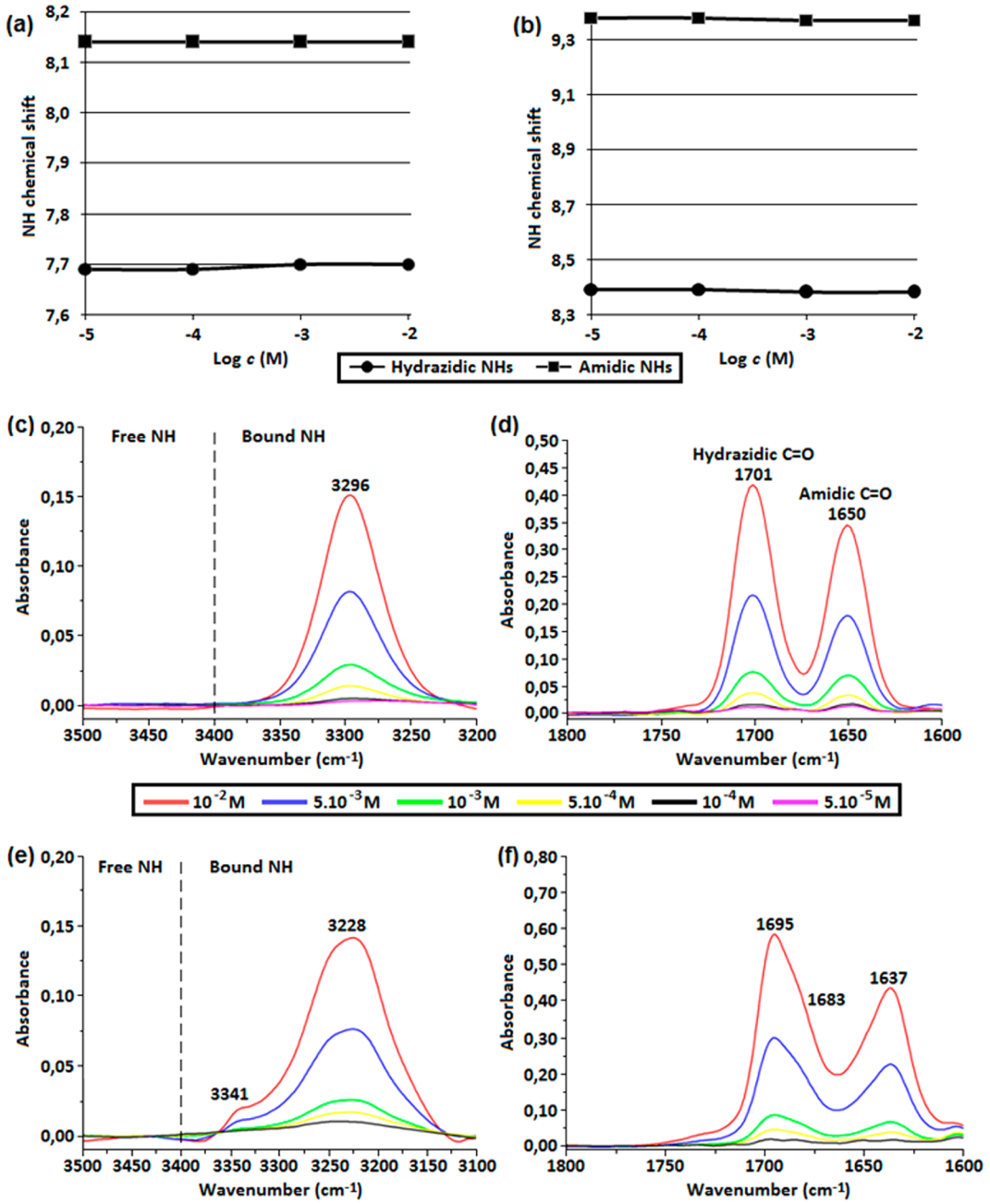

Figure 3. (a, b) Concentration-dependent ^{1}H NMR (300 MHz) chemical shifts in $CDCl_3$ (from 10^{-2} to 10^{-5} M) of (a) **3** and (b) **4**. (c–f) IR spectra in $CHCl_3$ of (c, d) **3** (from 10^{-2} M to 5.10^{-5} M) and (e, f) **4** (from 10^{-2} M to 10^{-4} M).

the literature.[5,26] In addition, the carbonyl groups, alternatively up and down, are oriented along the C_2 symmetry axis of the ring. Analysis of the α-CTP or α,β-CTP structures deposited in the Cambridge Structural Database (version 5.34) revealed that one-half or less of the carbonyl groups are oriented along the ring axis. In our case, the alignments of the carbonyl groups allow self-assembly of the molecules in a straight line. Indeed, each C═O group is involved in a bifurcated H-bond with one N−H and one C^{α}−H group. This tight packing is similar to that observed in cyclotetraurea peptides, where each bifurcated H-bond involves in this case both N−H groups of the urea bond.[13] Finally, the nanotubular rods are held together by CH−π and Van Der Walls interactions.

In the solid state, the amide N−H and C═O bonds are aligned parallel to the tube length while the side chains project pseudoequatorially from the exterior walls of the so-formed nanotubes. The crystal structure revealed that the molecule exists in a C_2-symmetric conformation in which the central hole of the peptide ring is collapsed and not large enough to accommodate water and small ions (Figure 2).[10,19] In contrast, the conformation adopted by the cyclo α-N^{α}-Bn-aza-β^3 tetramer in the solid state is quite different.[18] The latter assumes a monomeric form where all of the N−H and C═O bonds are involved in strong intramolecular hydrazinoturns. No tubular structure was observed. This result demonstrates that the presence of α-amino acid units in the cycle contributes to decreasing the strength of the intramolecular H-bonds and allows intermolecular interactions between NH and CO groups.

DOI: 10.1021/jo502684g
J. Org. Chem. 2015, 80, 3022−3029

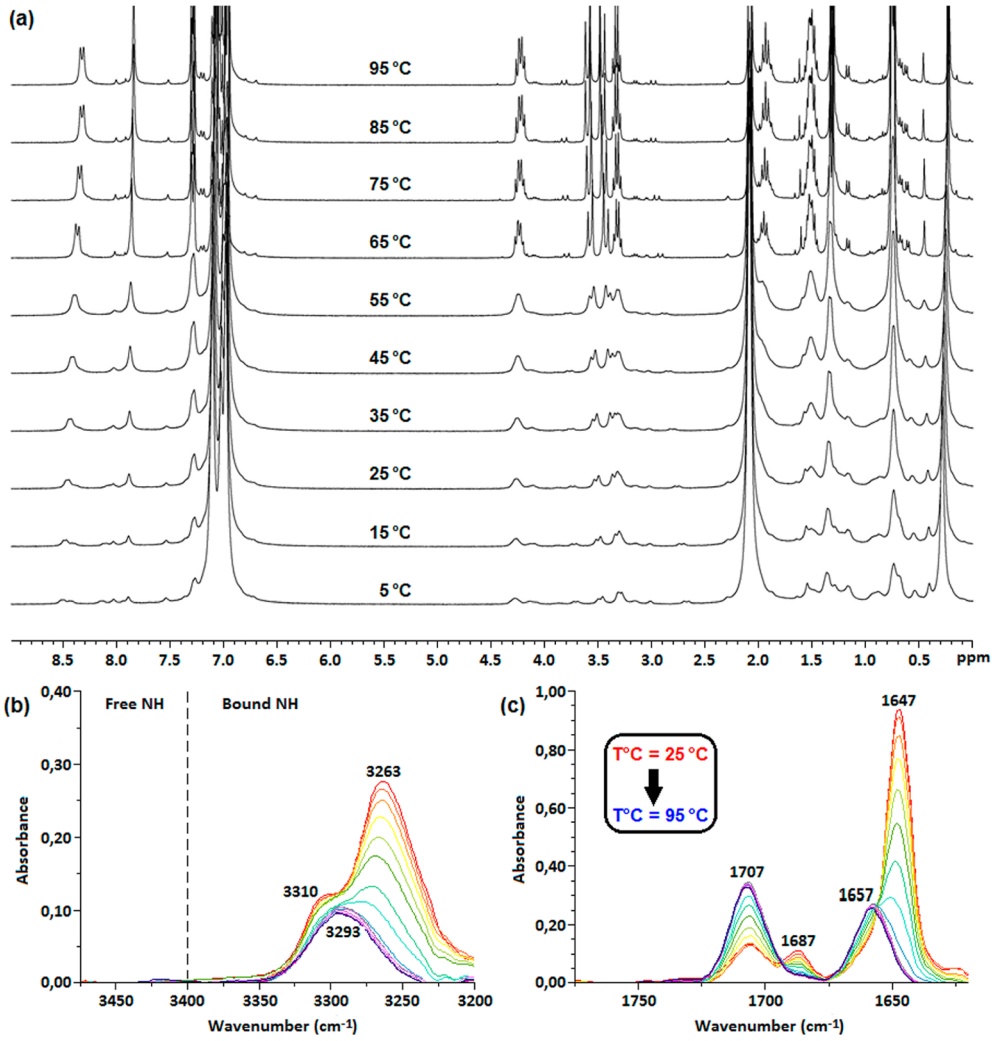

Figure 4. Temperature-dependent spectra of **3** in the gel state (toluene-d_8, $c = 8.6 \times 10^{-3}$ M): (a) ^{1}H NMR (300 MHz) spectra (from 5 to 95 °C); (b, c) FTIR spectra of **3** in $CHCl_3$ (from 25 to 95 °C).

Unfortunately, the X-ray structure of **4** could not be solved because of the poor quality of the crystals.

Concentration-dependent NMR and FTIR studies of **3** performed in $CDCl_3$ and $CHCl_3$, respectively, demonstrated that the nanotubular structure is not maintained in these solvents. A single signal could be detected for both hydrazidic and both amidic NHs, located at 7.7 and 8.1 ppm, respectively. This result was in agreement with a C_2-symmetric conformation. The high values of these chemical shifts seemed also to indicate that all of the NH protons were involved in a H-bonding network. In addition, these chemical shifts were not affected by a variation of the concentration (Figure 3a), demonstrating the absence of intermolecular H-bonds. 2D NMR analyses (see p S4 in the Supporting Information) led us to detect two types of intramolecular H-bond networks: a hydrazinoturn involving amidic NH and hydrazidic CO and a γ-turn involving hydrazidic NH and amidic CO (see Figure 1).

The intramolecular H-bonding network was further confirmed by FTIR measurements in $CHCl_3$ (Figure 3c,d). The N−H stretching band of **3** was below 3400 cm^{-1}, centered at 3296 cm^{-1}. This observation suggested the existence of a H-bonding network in which all of the NH protons were involved.[27] In the CO area, two bands were detected at 1650 and 1701 cm^{-1}, assigned respectively to bonded amidic CO and bonded hydrazidic ones. Furthermore, these wavenumbers were constant with varying concentrations of **3** in $CHCl_3$, confirming the exclusive presence of intramolecular H-bonding contacts.

Similar to what was observed for compound **3**, ^{1}H NMR and FTIR experiments in $CDCl_3$ and $CHCl_3$ demonstrated that compound **4** did not self-assemble in $CHCl_3$ and that all of the NH protons were involved in an intramolecular H-bonding network (Figure 3b,e,f). Thus, we can conclude that compound **4** did not adopt a tubular structure in solution.

When a small amount of **3** was refluxed and cooled in toluene or dodecane, the formation of a thermoreversible physical organogel was observed. Thermoreversible physical organogels are the consequence of self-assembly of molecules into fibers that trap the solvent by forming a three-dimensional network through noncovalent cross-linked interactions.[28] The sol to gel transition can be monitored by measuring the elastic modulus (storage modulus G') and viscous modulus (loss modulus G'') at a certain frequency as a function of temperature. The rheogram on p S5 in the Supporting Information shows the viscous (G'') and elastic (G') response behavior of **3** in toluene-d_8 solution at the critical gelation concentration (8.6×10^{-3} M) as a function of temperature.

DOI: 10.1021/jo502684g
J. Org. Chem. 2015, 80, 3022−3029

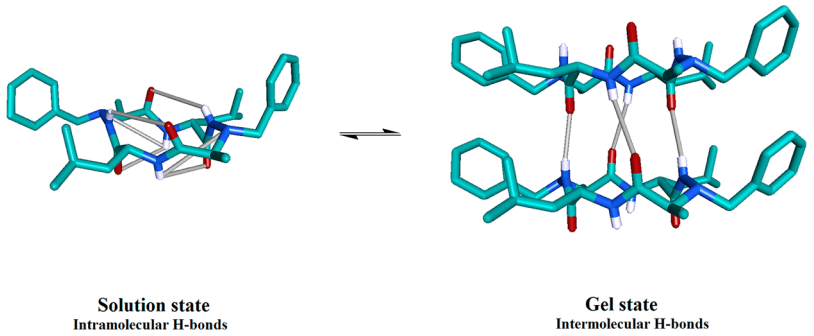

Figure 5. Representation of the equilibrium between intramolecular (solution state) and intermolecular (gel state) H-bonds of **3** in toluene-d_8. The H atoms, except those of the NH groups, have been omitted for clarity.

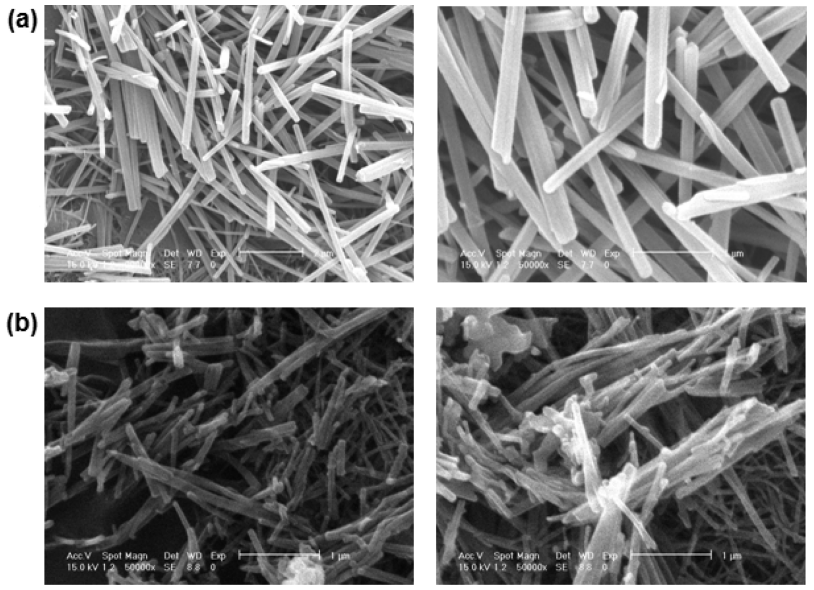

Figure 6. SEM images of aerogels obtained from organogels of (a) **3** in toluene (external diameters of the fibers were measured to be around 220 nm) and (b) **4** in cyclohexane (external diameters of the fibers were measured to be around 150 nm).

This graph shows the gel formation point of **3** (the intersection of the G' and G'' curves) at around 62 °C.

To gain further insight into these phenomena, the behavior of **3** in toluene-d_8 was then investigated using temperature-dependent FTIR and NMR spectroscopy from 25 °C (gel state) to 95 °C (solution state) (Figure 4). FTIR measurements at 25 °C showed the presence of two N−H stretching bands characteristic of H-bonded NH groups located respectively at 3310 and 3263 cm^{-1}. Heating the toluene-d_8 gel of **3** from 5 to 95 °C led to a gradual collapse of the H-bonded NH in favor of one band located at 3293 cm^{-1}, as shown in Figure 4b. This observation could be interpreted as the consequence of the disruption of the intermolecular H-bonding network responsible for the gel formation. This wavenumber was close to the one obtained in $CHCl_3$ and was characteristic of an intramolecular H-bonded NH (Figure 4b). Studies of the C═O stretching bands gave rise to the same conclusion. Four H-bonded CO, located at 1647, 1658, 1687, and 1707 cm^{-1} (see the deconvolution spectra on p S7 in the Supporting Information), could be observed in the gel state (red, Figure 4c). Heating the solution led to the collapse of the bands located at 1647 and 1687 cm^{-1} in favor of the peaks located at 1657 and 1707 cm^{-1}. The shape of the spectra recorded at high temperatures was very similar to the one obtained for **3** in $CHCl_3$. In agreement with the results obtained for the NH signals, we can conclude that the bands located at 1657 and 1707 cm^{-1} corresponded to intramolecular H-bonded amidic and hydrazidic CO, respectively, and those located at 1647 and 1687 cm^{-1} to intermolecular H-bonded amidic and hydrazidic CO, respectively.

In most of the cases reported in the literature, the gelator NMR signals completely disappear in the gel state but are present in the liquid state.[29] This observation can be explained by the fact that the gel fiber can be considered as a crystal of the gelator in which the molecular motion is very limited and the solvent molecules are excluded from the fibers. Therefore, the disappearance of the ^{1}H NMR peaks is considered to be one criterion for "dry gels". In our case, the lower the temperature, the lower the visible part of the molecule in the ^{1}H NMR spectrum (Figure 4a). However, peaks were always detected, even at 5 °C. This result suggests that some of the gelator molecules still kept good thermal mobility in the fibers.[28,30] The chemical shifts of the gelator signals were unchanged when the temperature was varied, demonstrating that the free and aggregate species were separated.[31]

The ^{1}H NMR spectra of the gel in toluene-d_8 displayed signals that were quite different from the ones obtained in $CDCl_3$ at the same temperature. In the gel state (from 5 to 50 °C), several signals could be observed for hydrazidic and amidic NHs around 7.9 and 8.4 ppm, respectively. A coalescence

DOI: 10.1021/jo502684g
J. Org. Chem. 2015, 80, 3022−3029

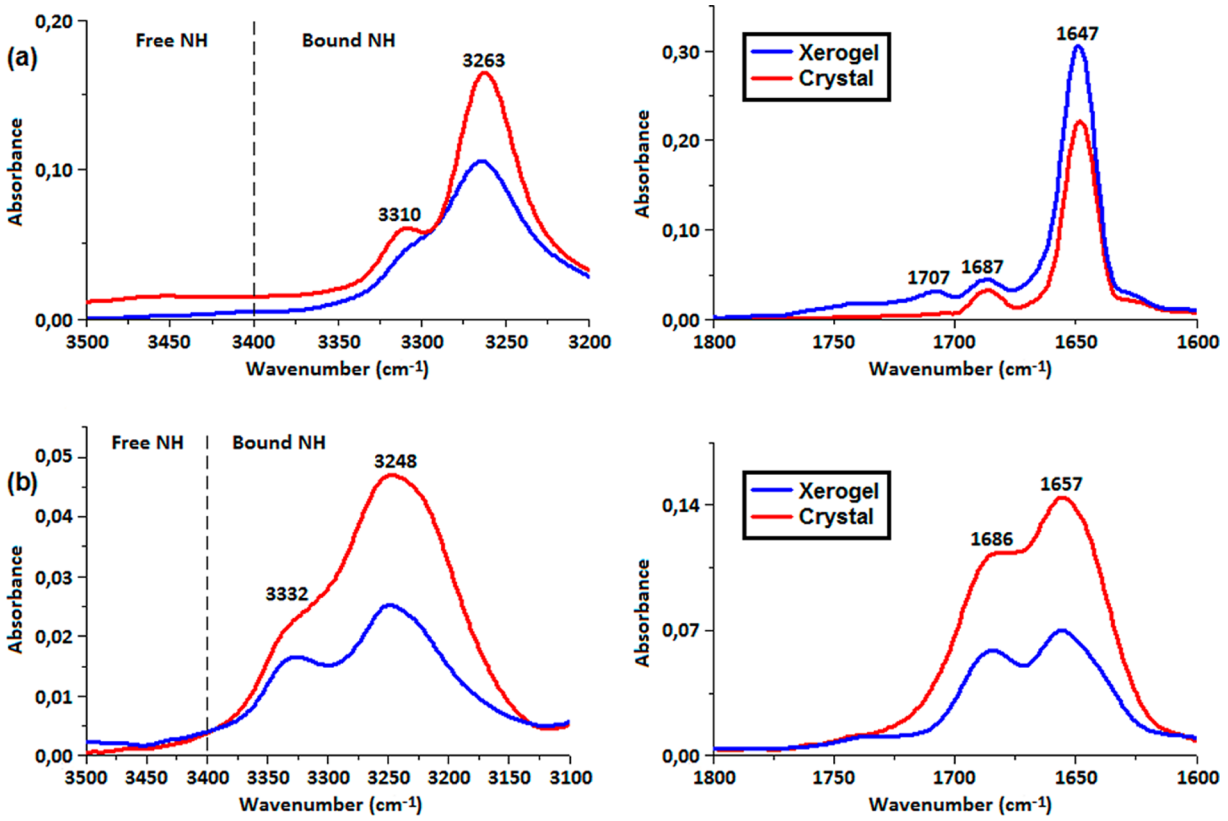

Figure 7. Comparison of the ATR-FTIR spectra in the crystal and xerogel states for (a) **3** and (b) **4**.

phenomenon occurred when the temperature reached 50 °C. We and others had already observed this phenomenon and concluded that the NMR-visible part of the gel could be composed of monomers but also of incipient precursors corresponding to small associated species.[28a,32] Over 55 °C, the gel turned into a solution, and its spectrum looked like the one obtained in $CDCl_3$, with the presence of a unique set of signals for amidic and hydrazidic NHs. Heating the gel finally led to total molecular dissociation.

All of these observations are in agreement with the presence of a slow equilibrium between monomeric and nanotubular forms in the gel state (Figure 5). These nanotubes could be associated through $\pi-\pi$ stacking interactions between the aromatic segments in the gel.

The removal of all of the solvent using a supercritical CO_2 drying process led to the formation of the corresponding aerogel[33] (see p S11 in the Supporting Information). SEM analysis performed on this dried material confirmed the presence of nontwisted fibers (Figure 6a). The diameter of these fibers was evaluated to be around 220 nm.

Comparison of the ATR-FTIR spectra of the xerogel (obtained by slow evaporation of the organogel state in air) and the crystal showed the presence of two N−H stretching bands located at 3263 and 3310 cm^{-1} and two small CO stretching bands at 1647 and 1687 cm^{-1} (Figure 7a). In agreement with the previous results, small bands located at 1657 cm^{-1} (see the deconvolution spectra on p S8 in the Supporting Information) and 1707 cm^{-1} could also be detected in the xerogel, both corresponding to intramolecular CO H-bonds. The similarity between these spectra led us to conclude that the same nanotubular structure exists in the crystal and the xerogel and by deduction in the organogel. The presence of a nanotubular structure in the gel state was also demonstrated by powder X-ray diffraction (XRD) analysis. The XRD data for the aerogel of **3** exhibited a stacking pattern that was very similar to the one observed in the crystal structure, indicating that the molecules in the gel state adopted a similar packing mode (nanotubular structure) as in the crystal structure (Figure 8).

Interestingly, an organogel of **4** could be obtained only in cyclohexane and was transformed into the corresponding aerogel. SEM analysis confirmed also the presence of

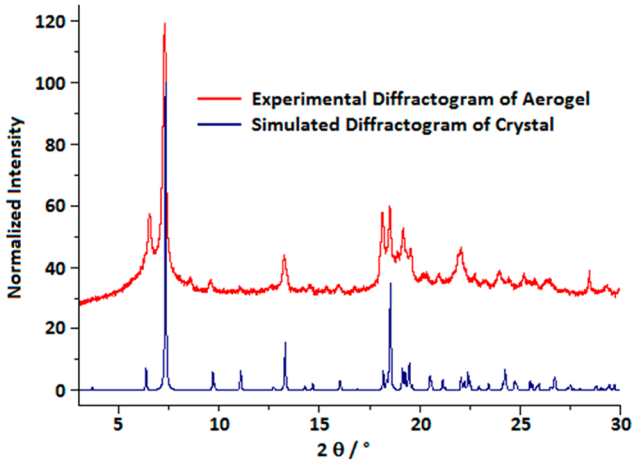

Figure 8. XRD patterns of the aerogel of **3** (red) and the theoretical profile calculated from its crystallographic data (blue). The powder XRD measurement was performed using a diffractometer equipped with a Cu tube and a Ge(111) incident-beam monochromator (λ = 1.5406 A). Data collection was carried out over the scattering angle (θ) range of 3−55° in steps of 0.0167° over 15 h.

DOI: 10.1021/jo502684g
J. Org. Chem. 2015, 80, 3022−3029

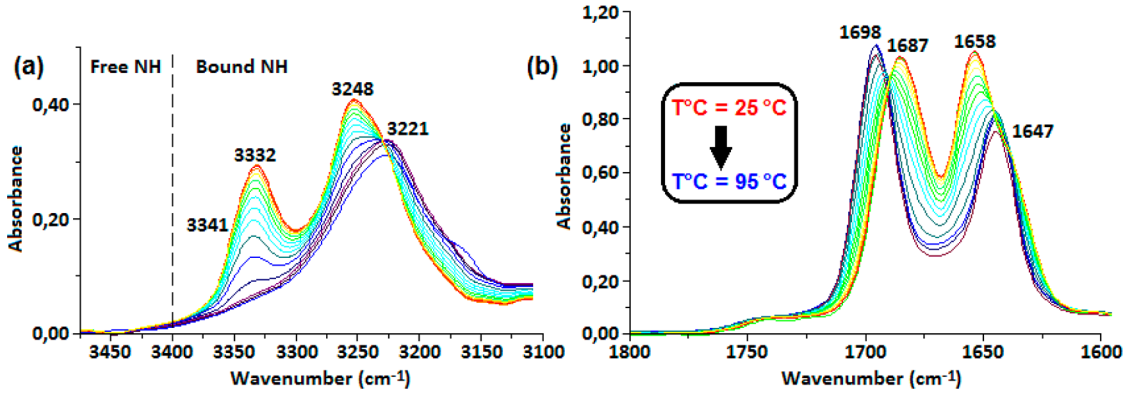

Figure 9. Temperature-dependent IR spectra from 25 to 95 °C of **4** in the gel state (cyclohexane, $c = 8.6 \times 10^{-3}$ M).

nontwisted fibers (Figure 6b). In the case of compound **4**, the diameter of the fibers (150 nm) was smaller than that observed for compound **3** (220 nm). As shown in Figure 9, FTIR spectra recorded for the organogel of **4** in cyclohexane at different temperatures demonstrated that heating the cyclohexane organogel from 25 to 95 °C led to a gradual collapse of the NH bands located at 3332 and 3248 cm^{-1} in favor of one located at 3221 cm^{-1}. This last band was located much closer to those obtained in $CHCl_3$ and should correspond to the signature of nonassembled molecules. Moreover, comparison of the ATR-FTIR spectra of the xerogel and the crystal demonstrated the same IR signature for the two states (Figure 7b). All of these results led us to conclude that compound **4** was self-assembled in the same manner in the gel and in the crystal state.

CONCLUSION

The present work emphasizes the synthesis of new mixed cyclic 1:1 [α/α-N^{α}-Bn-hydrazino]mers and their ability to adopt two types of self-assembly in solution, the solid state, and the gel phase. While **3** and **4** fold into an intramolecular H-bonding network through alternate γ-turns and hydrazinoturns in the same way as their linear counterparts in chloroform, they are also able to self-assemble into an intermolecular H-bond network to form thermoreversible physical organogels. This self-assembly occurs in specific solvents, namely, toluene and cyclohexane for **3** and **4**, respectively. Removal of the solvent by a supercritical CO_2 process gives access to the corresponding aerogels, which reveal the existence of nontwisted fibers through SEM analysis. The intermolecular H-bonding network responsible for the gel formation seems to arise from nanotubular self-organization, as demonstrated by the X-ray crystallographic structure of **3**. It is noteworthy that for **3**, the xerogel, the organogel, and the crystal present the same IR signature and XRD pattern, thus confirming that nanotubes also exist in solution and in the gel. Therefore, since obtaining an organogel in cyclohexane for compound **4** is in agreement with the presence of self-organization, we expect nanotube formation within the molecules.

EXPERIMENTAL SECTION

General. Unless otherwise stated, all chemicals were purchased as the highest purity commercially available and were used without further purification. Dry DCM was obtained by distillation over P_2O_5 under an argon atmosphere, MeOH was purchased in anhydrous form, and other reagent-grade solvents were used as received.

Reactions were monitored by thin-layer chromatography (TLC) using aluminum-backed silica gel plates. TLC spots were viewed under UV light or/and by heating the plate after treatment with a staining solution of phosphomolybdic acid. Chromatography was carried out on silica gel (0.04–0.063 μm). All yields were calculated from pure isolated products.

^1H and ^{13}C NMR spectra were recorded on a 300 MHz spectrometer. Chemical shifts (δ) are given in parts per million relative to tetramethylsilane (TMS), and coupling constants (J) are given in hertz. The spectra were recorded in $CDCl_3$ solvent at room temperature. TMS served as an internal standard (δ = 0 ppm) for ^1H NMR, and $CDCl_3$ was used as an internal standard (δ = 77.0 ppm) for ^{13}C NMR. Multiplicities are reported as follows: s = singlet, d = doublet, q = quartet, m = multiplet, br = broad, Ar. = aromatic. IR spectra were recorded over 256 scans. Electrospray ionization mass spectrometry (ESI-MS) was performed on a ToF-Q HR spectrometer. HRMS spectra were obtained by the ESI method. All melting points (mp) were measured and are uncorrected.

General Ester Deprotection Procedure. To a solution of methyl ester-protected **1** or **2** (1.0 equiv, 22 mmol) in MeOH (80 mL) was added a solution of 1 N NaOH (2.0 equiv, 44 mmol) at 0 °C. The mixture was vigorously stirred for 3–6 h at room temperature until reaction completion (as monitored by TLC). After evaporation of MeOH, the aqueous layer was washed with cyclohexane (2 × 10 mL). The aqueous phase was cooled to 0 °C and acidified with 1 N HCl to pH 1 and extracted with EtOAc (3 × 20 mL). The residue was dried over $MgSO_4$, filtered, and evaporated *in vacuo* to give the corresponding carboxylic acid, which was used without further purification.

General Boc Deprotection and Macrocyclization Procedures. To a stirred solution of a Boc-protected compound (1.0 equiv, 9 mmol) in DCM was added a portion of TFA representing two-thirds of the quantity of DCM added. The mixture was stirred overnight without any control by TLC. The solution was concentrated under vacuum, and the excess of TFA was coevaporated with MeOH and Et_2O, affording the corresponding trifluoroacetate salt compound as a white foam in quantitative yield. The crude residue was dissolved in DCM, and DIPEA was added (4.0 equiv, 36 mmol). The solution was added dropwise into a solution of HBTU (1.0 equiv, 9 mmol) in DCM (the concentration was almost 1 mM in the mixture). This slow addition ran during 7 h, and then the reaction mixture was stirred at room temperature under nitrogen for 2 days. The volume was reduced to around 100 mL, and the solution was washed successively with 1 N HCl (2 × 20 mL), saturated $NaHCO_3$ (2 × 20 mL), H_2O (2 × 20 mL), and brine (2 × 20 mL) and finally dried over $MgSO_4$ and evaporated in vacuo to give **3** or **4** as a white solid. The resulting crude material was purified and characterized as reported below.

Heterochiral Cyclotetramer [L-Leucine-N^{α}-benzyl-D-hydrazinoalanine]$_2$ (3). White powder (2.08 g, 40%). Purified by precipitation with Et_2O/MeOH. Characterization data: mp 327 °C; ^1H NMR (300 MHz, $CDCl_3$, 10 mM) δ 0.75 (d, J = 6.3 Hz, 6H, 2 δ-CH_3 Leu), 0.78 (d, J = 6.3 Hz, 6H, 2 δ-CH_3 Leu), 1.32 (d, J = 6.9 Hz,

DOI: 10.1021/jo502684g
J. Org. Chem. 2015, 80, 3022–3029

6H, 2 β-CH_3 Ala), 1.33−1.50 (m, 4H, 2 γ-CH Leu, 1 β-CH_2 Leu), 1.58−1.82 (m, 2H, 1 β-CH_2 Leu), 3.42 (q, J = 6.9 Hz, 2H, 2 α-CH Ala), 3.76 (d, J = 12.3 Hz, 2H, CH_2 N^{α}-Bn), 3.84 (d, J = 12.3 Hz, 2H, CH_2 N^{α}-Bn), 4.10 (dd, J = 16.2 and 7.2 Hz, 2H, 2 α-CH Leu), 7.16−7.28 (m, 6H, Ar.), 7.30−7.38 (m, 4H, Ar.), 7.70 (s, 2H, 2 hydrazidic NHs), 8.14 (d, J = 9.3 Hz, 2H, 2 amidic NHs); ^{13}C NMR (75 MHz, $CDCl_3$) δ 6.7 (2 β-CH_3 Ala), 23.2 (4 δ-CH_3 Leu), 25.4 (2 γ-CH Leu), 37.3 (2 β-CH_2 Leu), 49.6 (2 α-CH Leu), 59.4 (2 α-CH Ala), 60.7 (2 CH_2, N^{α}-Bn), 128.7 (2 CH Ar.), 129.2 (4 CH Ar.), 130.0 (4 CH Ar.), 136.6 (2 C Ar.), 170.9 (2 C═O hydrazide), 173.5 (2 C═O amide); HRMS (ESI) calcd for $C_{32}H_{46}N_6O_4$ $[M + Na]^+$ m/z 601.3478, found 601.3473.

Heterochiral Cyclohexamer [L-Leucine-N^{α}-benzyl-D-hydrazinoalanine]$_3$ (4). White powder (3.13 g, 35%). Purified by flash chromatography with EtOAc/MeOH = 95:5. Characterization data: mp 163 °C; ^{1}H NMR (300 MHz, $CDCl_3$, 10 mM) δ 0.80 (d, J = 6.3 Hz, 9H, 3 δ-CH_3 Leu), 0.87 (d, J = 7.2 Hz, 9H, 3 δ-CH_3 Leu), 1.13 (d, J = 7.2 Hz, 9H, 3 β-CH_3 Ala), 1.51−1.69 (m, 9H, 3 γ-CH Leu, 3 β-CH_2 Leu), 3.43 (q, J = 7.2 Hz, 3H, 3 α-CH Ala), 3.82−3.99 (m, 9H, 3 CH_2 N^{α}-Bn, 3 α-CH Leu), 7.18−7.39 (m, 15H, Ar.), 8.38 (s, 3H, 3 hydrazidic NHs), 9.37 (br d, J = 5.4 Hz, 3H, 3 amidic NHs); ^{13}C NMR (75 MHz, $CDCl_3$) δ 12.3 (3 β-CH_3 Ala), 22.7 (3 δ-CH_3 Leu), 23.6 (3 δ-CH_3 Leu), 25.2 (3 γ-CH Leu), 37.6 (3 β-CH_2 Leu), 50.8 (3 α-CH Leu), 60.9 (3 CH_2 N^{α}-Bn), 62.4 (3 α-CH Ala), 128.6 (3 CH Ar.), 129.1 (6 CH Ar.), 129.9 (6 CH Ar.), 136.7 (3 C Ar.), 173.0 (3 C═O hydrazide), 175.6 (3 C═O amide); HRMS (ESI) calcd for $C_{48}H_{69}N_9O_6$ $[M + Na]^+$ m/z 890.5269, found 890.5263.

■ ASSOCIATED CONTENT

Ⓢ Supporting Information

Copies of ^{1}H and ^{13}C NMR spectroscopic data for compounds **3** and **4**, portion of the 2D NOESY NMR spectroscopic data and rheological data for compound **3**, IR and ATR-FTIR spectra (deconvolution) for compound **3** in the gel state (solution and xerogel, respectively), crystallographic data (CIF) for compound **3**, and method of aerogel preparation. This material is available free of charge via the Internet at http://pubs.acs.org.

■ AUTHOR INFORMATION

Corresponding Authors

*E-mail: Samir.Acherar@univ-lorraine.fr.

*E-mail: Brigitte.Jamart@univ-lorraine.fr.

Notes

The authors declare no competing financial interest.

■ ACKNOWLEDGMENTS

The authors acknowledge O. Fabre for running NMR experiments and E. Wenger for performing XRD experiments.

■ REFERENCES

(1) Duncan, R.; Gaspar, R. *Mol. Pharmaceutics* **2011**, *8*, 2101.
(2) Lin, Y.; Taylor, S.; Li, H.; Fernando, K. A. S.; Qu, L.; Wang, W.; Gu, L.; Zhou, B.; Sun, Y.-P. *J. Mater. Chem.* **2004**, *14*, 527.
(3) Martin, C. R.; Kohli, P. *Nat. Rev. Drug Discovery* **2003**, *2*, 2.
(4) Hassall, C. H. *Chem. Biol. Pept., Proc. Am. Pept. Symp. 3rd* **1972**, 153.
(5) Karle, I. L.; Handa, B. K.; Hassall, C. H. *Acta Crystallogr.* **1975**, *B31*, 555.
(6) De Santis, P.; Morosetti, S.; Rizzo, R. *Macromolecules* **1974**, *7*, 52.
(7) Ghadiri, M. R.; Granja, J. R.; Milligan, R. A.; McRee, D. E.; Khazanovich, N. *Nature* **1993**, *366*, 324.
(8) Jagannadh, B.; Reddy, M. S.; Rao, C. L.; Prabhakar, A.; Jagadeesh, B.; Chandrasekhar, S. *Chem. Commun.* **2006**, 4847.
(9) Fujimura, F.; Hirata, T.; Morita, T.; Kimura, S.; Horikawa, Y.; Sugiyama, J. *Biomacromolecules* **2006**, *7*, 2394.
(10) Seebach, D.; Matthews, J. L.; Meden, A.; Wessels, T.; Baerlocher, C.; McCusker, L. B. *Helv. Chim. Acta* **1997**, *80*, 173.
(11) Gademann, K.; Ernst, M.; Hoyer, D.; Seebach, D. *Angew. Chem., Int. Ed.* **1999**, *38*, 1223.
(12) Gauthier, D.; Baillargeon, P.; Drouin, M.; Dory, Y. L. *Angew. Chem., Int. Ed.* **2001**, *40*, 4635.
(13) Semetey, V.; Didierjean, C.; Briand, J.-P.; Aubry, A.; Guichard, G. *Angew. Chem., Int. Ed.* **2002**, *41*, 1895.
(14) Fischer, L.; Decossas, M.; Briand, J.-P.; Didierjean, C.; Guichard, G. *Angew. Chem., Int. Ed.* **2009**, *48*, 1625.
(15) Günther, R.; Hofmann, H.-J. *J. Am. Chem. Soc.* **2001**, *123*, 247.
(16) Lelais, G.; Seebach, D. *Helv. Chim. Acta* **2003**, *86*, 4152.
(17) Le Grel, P.; Salaün, A.; Potel, M.; Le Grel, B.; Lassagne, F. *J. Org. Chem.* **2006**, *71*, 5638.
(18) Salaün, A.; Mocquet, C.; Perochon, R.; Lecorgne, A.; Le Grel, B.; Potel, M.; Le Grel, P. *J. Org. Chem.* **2008**, *73*, 8579.
(19) Clark, T. D.; Buehler, L. K.; Ghadiri, M. R. *J. Am. Chem. Soc.* **1998**, *120*, 651.
(20) (a) Acherar, S.; Salaün, A.; Le Grel, P.; Le Grel, B.; Jamart-Grégoire, B. *Eur. J. Org. Chem.* **2013**, 5603. (b) Moussodia, R.-O.; Acherar, S.; Bordessa, A.; Vanderesse, R.; Jamart-Grégoire, B. *Tetrahedron* **2012**, *68*, 4682.
(21) Yang, D.; Ng, F.-F.; Li, Z.-J.; Wu, Y.-D.; Chan, K. W. K.; Wang, D.-P. *J. Am. Chem. Soc.* **1996**, *118*, 9794.
(22) Yang, D.; Li, W.; Qu, J.; Luo, S.-W.; Wu, Y.-D. *J. Am. Chem. Soc.* **2003**, *125*, 13018.
(23) Acherar, S.; Jamart-Grégoire, B. *Tetrahedron Lett.* **2009**, *50*, 6377.
(24) Salaün, A.; Potel, M.; Roisnel, T.; Gall, P.; Le Grel, P. *J. Org. Chem.* **2005**, *70*, 6499.
(25) Salaün, A.; Favre, A.; Le Grel, B.; Potel, M.; Le Grel, P. *J. Org. Chem.* **2006**, *71*, 150.
(26) (a) Hass, K.; Ponikwar, W.; Nöth, H.; Beck, W. *Angew. Chem., Int. Ed.* **1998**, *37*, 1086. (b) Di Blasio, B.; Lombardi, A.; D'Auria, G.; Saviano, M.; Isernia, C.; Maglio, O.; Pedone, L.; Pavone, V. *Biopolymers* **1993**, *33*, 621.
(27) Formaggio, F.; Crisma, M.; Toniolo, C.; Broxterman, Q. B.; Kaptein, B.; Corbier, C.; Saviano, M.; Palladino, P.; Benedetti, E. *Macromolecules* **2003**, *36*, 8164.
(28) (a) Allix, F.; Curcio, P.; Pham, Q. N.; Pickaert, G.; Jamart-Grégoire, B. *Langmuir* **2010**, *26*, 16818. (b) Van Esch, J. H. *Langmuir* **2009**, *25*, 8392. (c) Hanabusa, K.; Yamada, M.; Kimura, M.; Shirai, H. *Angew. Chem., Int. Ed. Engl.* **1996**, *35*, 1949.
(29) Cassin, G.; De Costa, C.; Van Duynhoven, J. P. M.; Agterof, W. G. M. *Langmuir* **1998**, *14*, 5757.
(30) (a) Sakurai, K.; Jeong, Y.; Koumoto, K.; Friggeri, A.; Gronwald, O.; Sakurai, S.; Okamoto, S.; Inoue, K.; Shinkai, S. *Langmuir* **2003**, *19*, 8211. (b) Wang, R.; Geiger, C.; Chen, L.; Swanson, B.; Whitten, D. G. *J. Am. Chem. Soc.* **2000**, *122*, 2399. (c) Geiger, C.; Stanescu, M.; Chen, L.; Whitten, D. G. *Langmuir* **1999**, *15*, 2241.
(31) Escuder, B.; Llusar, M.; Miravet, J.-F. *J. Org. Chem.* **2006**, *71*, 7747.
(32) Duncan, D. C.; Whitten, D. G. *Langmuir* **2000**, *16*, 6445.
(33) Placin, F.; Desvergne, J.-P.; Cansell, F. *J. Mater. Chem.* **2000**, *10*, 2147.

DOI: 10.1021/jo502684g
J. Org. Chem. 2015, 80, 3022−3029